FEMS Microbiology Ecology 12 (1993) 237–248

Published by Elsevier

FEMSEC 00471

Nucleic acids from the host bacterium as a major source of nucleotides for three marine bacteriophages

J. Wikner [b], J.J. Vallino [a], G.F. Steward [a], D.C. Smith [a] and F. Azam [a]

[a] *Scripps Institution of Oceanography, UCSD, La Jolla, CA, USA, and* [b] *Department of Microbiology, Umeå University, Umeå, Sweden*

(Received 23 December 1992; revision received 11 May 1993; accepted 17 May 1993)

Abstract: The incorporation of ^{32}P-phosphorus into marine bacteriophage nucleic acid was studied in culture experiments to investigate the source of nucleotides used by the phage. We consistently found that the ^{32}P-specific activity in the phage genome increased during the 11 h incubation and was low relative to the specific activity in the medium, averaging 21% (±SD 5.9) for the three phage isolates. This was in accordance with a mathematical model where most of the nucleotides for phage DNA synthesis were derived from the host cell nucleic acid rather than de novo synthesis. We propose that this metabolic strategy may be common among marine phages, as an adaptation to a nutrient poor environment. Consequently, the contribution of free DNA to the dissolved fraction through phage lysis of bacteria, may be less that previously thought. Also during radiolabelling of bacteriophages in natural water samples, isotope dilution may be dependent on the specific growth rate of the bacterial host.

Key words: Marine; Bacteriophage; Growth; Phosphorus; Nucleotides; Radiolabeling

Introduction

Bacteriophages (phages) are abundant in the marine environment, and have the potential to cause significant mortality of pelagic bacteria [1,2]. The direct growth environment of bacteriophages is the cytoplasm of the host bacterium. Nucleotides for phage nucleic acid synthesis may be produced by either de novo synthesis or degradation of host nucleic acid, as observed for the enteric T-even phages [3]. Determining the origin of phage nucleotides would give information about the growth characteristics of marine phages, and to what extent bacterial DNA is incorporated into phage nucleic acid or enter the dissolved fraction as free DNA after cell lysis. In addition, the nucleotide metabolism of marine phages will have consequences for the accuracy of phage production estimates by radiolabelling of the phage genome [4].

In this paper we investigate the origin of the nucleotides in three marine phages by monitoring the specific activity of the phage DNA following growth of phage in medium supplemented with $^{32}PO_4^{3-}$. This approach is similar to that used to investigate the origin of nucleotides in the enteric phage T4r$^+$ ([5], and references therein). To aid the interpretation of our results we developed a

Correspondence to: J. Wikner, Department of Microbiology, Umeå University, S-901 87, Umeå, Sweden.

computer model to simulate the specific activity of phage DNA with or without degradation of the host genome. The nucleotide metabolism observed is discussed in the context of adaptation to the marine environment and the consequences for measurement of in situ phage production are considered.

Materials and Methods

Strains and media

Marine phage-host systems (PHSs) were isolated from sea water collected off Scripps Pier and are designated MØ21/50, MØ21/43 and MØ14/67 (Steward et al., unpublished data).

The growth medium used in the culture experiments was 800 ml 0.45 μm filtered sea water and 200 ml distilled water amended with 0.05 g NH_4Cl, 0.02 g $MgCl_2 \cdot 6H_2O$, 0.01 g $K_2HPO_4 \cdot 3H_2O$, 0.6 mg Ferric citrate and 1.0 g Tryptone (Difco) (SWM). The concentration of molybdate reactive phosphorus in this medium was determined according to Parsons et al. [6]. Phosphate buffer (1 × PBA) (0.025 M $NaH_2PO_4 \cdot H_2O$, 0.001 M $MgCl_2 \cdot 6H_2O$, pH 3.5, dissolved in distilled water) was used for preparing saturated ammonium sulphate and resuspending pelleted viruses in the labelling experiments. Agarose gels were made and run in TBE pH 7.8 buffer (Tris base 0.089 M, boric acid 0.089 M, EDTA 0.002 M). Sample buffer (SB) was added to samples prior to gel electrophoresis (6x SB solution: 0.015 M $NaH_2PO_4 \cdot H_2O$, 0.001 M $MgCl_2 \cdot 6H_2O$, 40% sucrose (w/v), 0.25% bromphenol blue (w/v)). Carrier-free $^{32}PO_4^{3-}$ (314 TBq mmol^{-1}, > 99% radionucleotide purity, dissolved in water, New England Nuclear, cat. No. NEX-053) was used for the radiolabelling experiments.

Plaque assay

Plating cells were grown from the host strain according to Sambrook et al. [7]. Plating cells (0. 1 ml) were mixed with 0.1 ml of phage suspension, incubated 10 min at 21°C, and mixed with 3.5 ml of soft agar (0.5% agar in Zobell 2216 E medium) prior to spreading on a hard agar plate (1.5% agar in ZoBell 2216 E medium). Plates were incubated inverted at 16°C until plaques formed. Plates with 100 to 700 plaques were used to estimate the phage titer. Calibration of plaque forming units (PFU) versus transmission electron microscopy counts of phage particles indicated 72% plaquing efficiency for MØ21//50 under these conditions. The 95% confidence interval for the PFU estimates was less than $2\sqrt{n}$, where n equals the number of plaques counted, as based on the Poisson distribution [8].

Transmission electron microscopy

Samples from a stock culture of phage MØ21/50 were diluted in salt solution [4]. Harvesting of viruses was performed by ultracentrifugation directly onto transmission electronmicroscopy (TEM) specimen grids [2]. The grids (200-mesh Cu coated with carbon-stabilized Formvar film; Ted Pella[D]) were rendered hydrophylic by high-voltage glow discharge (50 kV for 60 s) under vacuum to aid homogenous dispersion on the grid. Air-dried grids were examined and the titre of phages determined in a Hitachi H-500 TEM operated at 100 kV and at a magnification of ×40,000 as described in Ref. 2.

Filtration recover

The recovery of phage particles was tested by seeding a sterile sea water sample with 3×10^3 ml^{-1} of the three different phage types. Subsamples (4 ml) were filtered through a syringe filter (Acrodisc® 0.2 μm). Phage titres prior and subsequent to filtration were determined by plaque assay for six replicate samples as described above.

The efficiency of the Acrodisc® 0.2 μm filter in removing bacterial cells was tested by comparing colony forming units (CFU) before and after filtration on a natural seawater sample.

Ammonium sulphate precipitation

Ammonium sulphate precipitation was employed to concentrate phage particles by a procedure modified from Ziai et al. [9]. Precipitation recovery for the three different phage types was determined by adding them to 50 ml autoclaved sea water at a final concentration of 3×10^3 phage ml^{-1}. Triplicate samples of 0.1 ml were

withdrawn for determination of the titre of the different phages as described above. Subsamples (900 μl) of the phage suspension were distributed into six microcentrifuge tubes. Bovine serum albumin (BSA) was added to 0.005% final concentration and 900 μl of saturated (21°C) ammonium sulphate solution was mixed with the sample. The effective ammonium sulphate concentration at 0°C was 63%. The samples were incubated on ice for 20 min and the precipitate pelleted by centrifugation for 20 min at 16000 $\times g$ and 4°C. The precipitate was washed once with 2 volumes of 50% saturated ammonium sulphate, incubated for 10 min on ice, and centrifuged again for 10 min as above. The final precipitates were dissolved in 900 μl sterile sea water, and the phage titre was determined by plaque assay as described above.

^{32}P labelling of bacteriophage in culture

Overnight seed cultures of host bacteria were grown in SWM. For an experiment with uniformly pre-labelled host cells, bacteria were grown overnight in the presence of $^{32}PO_4^{3-}$ (10 μCi ml^{-1}). A volume of the overnight culture containing 10^{10} bacteria was centrifuged (5000 $\times g$, 10 min) and cells resuspended in 1 ml SWM. Bacteriophage was added at a multiplicity of infection (m.o.i.) of 0.05 and incubated at 16°C for 10 min to allow adsorption of the phage to the host. The phage-host mixture was then diluted to 100 ml with SWM (16°C) in a 250 ml Erlenmeyer flask. Radiolabelled orthophosphate was added to a final concentration of 10 μCi ml^{-1} and the sample was incubated at 16°C on a shaker table (100 rpm). Subsamples of 900 μl were taken every hour and prepared for electrophoresis as described previously [4]. In brief, samples were filtered through a 0.2 μm Acrodisc® and incubated with a mixture of DNase 1 (1 U ml^{-1}), RNase (1 U ml^{-1}) and Micrococcal Nuclease (5 U ml^{-1}) for 1 h (21°C). The nuclease treated subsamples were Acrodisc® (0.2 μm) filtered a second time, precipitated with ammonium sulphate and resuspended in TBE pH 7.8. Samples (50 μl) for determination of phage abundance by plaque assay were taken from the same Erlenmeyer flask, diluted and plaque assayed against the appropriate host as described above.

Electrophoresis

Labelled macromolecules were separated by agarose gel electrophoresis [7]. Agarose (Fisher) gels (0.5%) were made in TBE pH 7.8 buffer, which was also used as running buffer. Samples were mixed with sample buffer (SB), and EDTA was added to 0.02 M final concentration to chelate any Mg^{2+} ions. Samples were heated for 10 min at 65°C prior to loading, to aid disintegration of phage particles and denature any secondary structures on the nucleic acid [7]. Gels were run at 100 mA (2.9 V cm^{-1}) for 600 mAh without cooling. As internal reference, CsCl-gradient purified stocks of the different phage types were processed and run simultaneously on the gel, to identify the labelled phage genome. Determination of the genome size of the phage isolates was done in a 0.3% agarose gel at 4°C, run for 2400 mAh, using λ *Hin*dIII digest (Sigma) and pBR328 5 kb ladder (Bio-Rad) as standards.

Staining and autoradiography of the gel

Gels were stained for DNA and RNA with ethidium-bromide (0.5 μg ml^{-1}) for 45 min [7]. Destaining was performed in deionized water. Agarose gels were dried at 80°C for 1 h in a gel dryer (Bio-Rad, Model 583) on Whatman 3 mm Chromatography paper. Gels were attached to a solid support and autoradiographed (Kodak, XAR-5). Radioactive bands on the dried gel were located using the autoradiogram as a guide, and excised. Gel pieces with radioactive bands were put in scintillation vials, 10 ml scintillation cocktail (Ecoscint®) added and samples counted to a 2% error level (LKB LS6000TA). Activity in the phage DNA bands was corrected for losses due to filtration and ammonium sulphate precipitation specifically for each phage isolate.

Model description

Background and application

A population model, based on modified equations previously applied to describe phage-host

interactions [10], was utilised to represent the dynamics of host bacteria and phage observed in the experimental system. Parameter values were tuned so that both kinetics and absolute densities of phage and host in the model, closely matched those observed in the experimental system (Table 1, Fig. 1). A compartmental sub-model, representing the cellular concentrations of ^{32}P-label in nucleotide and nucleic acid pools of the bacteria and phage, was coupled to the population sub-model to examine the origin of phosphorus in phage nucleic acid. Simulations were also run to examine the sensitivity of isotope dilution kinetics to perturbations in parameter values, and effects of isotope dilution on in situ estimates of phage production rates. The simulation program used was SIMNON (Engineering Software Concepts, Inc.)

Table 1

Model parameters and values

Symbol	Parameter (value)
$x_u(t)$	Concentration of uninfected bacteria
$x_i(t)$	Concentration of infected bacteria
$v(t)$	Concentration of virions
$r_v(t)$	Phage infection rate (Eqn. 4)
μ	Bacterial specific growth rate (0.05 h^{-1})
λ	Maximum viral infection rate (0.05 h^{-1})
k_v	Half saturation constant for viral infection rate (1.0×10^{7} virion ml^{-1})
m_u	Death or loss rate of uninfected bacteria (0 h^{-1})
m_i	Death or loss rate of infected bacteria (0 h^{-1})
m_v	Loss of phage particles (0 h^{-1})
ρ	Phage particles per bacteria (100 virion $cell^{-1}$)
τ	Phage latent period (2 h)
$P_{nu}(t)$	Concentration of ^{32}P-label in free nucleotide pool of uninfected bacteria
$P_{ni}(t)$	Concentration of ^{32}P-label in free nucleotide pool of infected bacteria
$P_{gu}(t)$	Concentration of ^{32}P-label in nucleic acid pool of uninfected bacteria
$P_{gi}(t)$	Concentration of ^{32}P-label in nucleic acid pool of infected bacteria
$P_{gv}(t)$	Concentration of ^{32}P-label in the phage genome
γ_{nb}	Free nucleotides in bacterial cell (4.4×10^{-9} nmol $cell^{-1}$)
γ_{gb}	Nucleotides in bacterial genome plus RNA (2.0×10^{-7} nmol $cell^{-1}$)
γ_{gv}	Nucleotides in phage genome, 50 kilo base pairs (1.7×10^{-10} nmol $cell^{-1}$)
σ	Fraction of external phosphate that is labelled with ^{32}P (1.75×10^{-5})
α	Fraction of bacterial genome degraded for phage production (0 to 1)

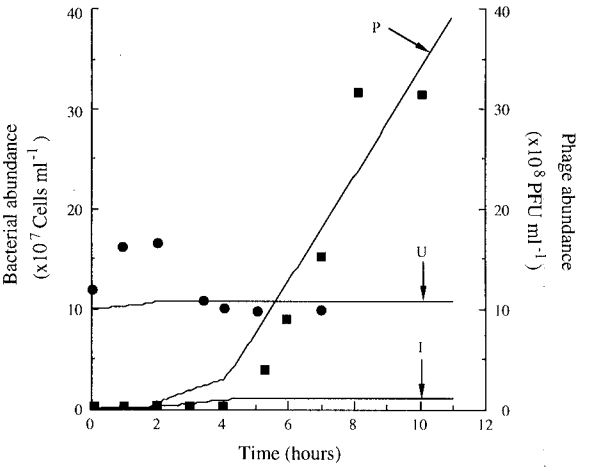

Fig. 1. Fit between simulated phage-host population dynamics and experimental data corresponding to Fig. 4A. Lines show expected dynamics of phage and bacteria based on the model. P; Phage population, U; uninfected bacterial population, I; infected bacterial population. Solid squares; phage 21/50 abundance, solid circles; bacterial abundance.

Definition of the population sub-model

The effects of host nucleic acid hydrolysis versus de novo nucleotide synthesis on the kinetics of phage ^{32}P-DNA specific activity was studied in a model developed to follow ^{32}P-label enrichment in the nucleotide and nucleic acid pools of bacteria and phage. The model consisted of two coupled state sub-models that describe (1) the population dynamics of the bacteria and phage, and (2) the ^{32}P-labelled nucleotide concentrations in five bacterial and phage compartments.

The population sub-model is given by

$$\frac{dx_u(t)}{dt} = \mu x_u(t) - r_v(t) - m_u x_u(t) \quad (1)$$

$$\frac{dx_i(t)}{dt} = r_v(t) - r_v(t-\tau)\, e^{-m_i\tau} - m_i x_i(t) \quad (2)$$

$$\frac{dv(t)}{dt} = \rho r_v(t-\tau)\, e^{-m_i\tau} - r_v(t) - m_v v(t) \quad (3)$$

is based on that described by Lenski [10], where the state variables $x_u(t)$, $t_i(t)$, and $v(t)$, represent

the concentrations (numbers per ml) of uninfected bacteria, infected bacteria and virions, respectively. Definitions of the other parameters are given in Table 1. Since resource limitations did not occur in the short batch experiments conducted, a resource variable was not included, and specific growth rate μ, was held constant. The function used by Lenski to describe phage infection rate, $r_v(t) = \lambda x_u(t) v(t)$, was found to produce unstable dynamics in the batch system and always resulted in collapse of the bacterial population. Since collapse of the bacterial population was never observed experimentally, the phage infection rate was modified to,

$$r_v(t) = \frac{\lambda x_u(t) v(t)}{v(t) + k_v} \tag{4}$$

so that the infection rate would saturate at high phage concentrations. This modified infection rate produced a stable system and also better matched the dynamics of phage production observed experimentally. The viral production rate at time t (first term Eqn. 3) was assumed to equal the infection rate at time $t - \tau$, times the viral burst size, ρ, where τ is the latent period for phage development, and the loss of infected bacteria before lysis is accounted for by the exponential term.

It was assumed that the viral burst size (ρ) was 100 [11,12] and that there were no bacterial or viral losses (other than phage induced lysis of infected cells) during the short incubations, so that the mortality terms (m_u, m_i and m_v) were set to be zero. The remaining parameters in the population sub-model (μ, λ, k_v, and τ) were tuned (Table 1), so that the simulated culture kinetics reflected those observed in the culture experiments (Fig. 1).

Definition of the phosphorus flux sub-model

To follow the kinetics of the phosphate label, five state variables were used to represent the concentration of ^{32}P-label (nmol ml^{-1}) in the free nucleotide pool of the infected and uninfected bacteria, $P_{nu}(t)$ and $P_{ni}(t)$, in the nucleic acid pool of the uninfected and infected bacteria, $P_{gu}(t)$ and $P_{gi}(t)$, and in the phage genome, $P_{gv}(t)$.

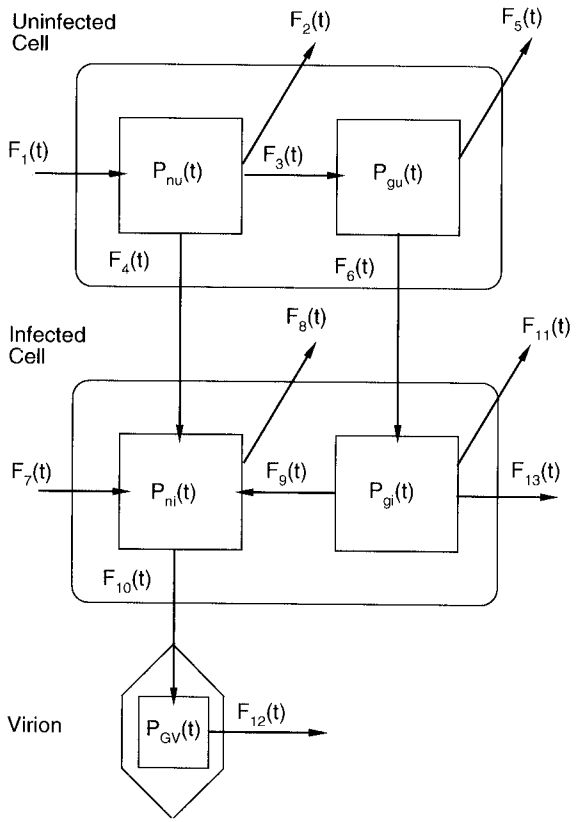

Fig. 2. Representation of ^{32}P-label in bacteria and phage nucleotide and nucleic acid pools. Balanced growth is assumed for uninfected bacteria. Nucleotides and nucleic acids in the infected bacteria are either excreted or synthesised (for nucleotides only), so that γ_{nb} and γ_{gb} remain constant. All pool concentrations in nmole ^{32}P-nucleotide ml^{-1}.

The connection between the five compartments are illustrated in Fig. 2, and the state equations were derived by constructing a label balance around each compartment. The flow of ^{32}P-label into a compartment is given by the total nucleotide flow into the compartment times the fraction of label in the flow, as given by:

$$\frac{dP_{nu}(t)}{dt} = \sigma F_1(t) - \frac{P_{nu}(t)}{\gamma_{nb} x_u(t)} (F_2(t) + F_3(t) + F_4(t)) \tag{5}$$

$$\frac{dP_{gu}(t)}{dt} = \frac{P_{nu}(t)}{\gamma_{nb} x_u(t)} F_3(t) - \frac{P_{gu}(t)}{\gamma_{gb} x_u(t)} \times (F_5(t) + F_6(t)) \tag{6}$$

$$\frac{dP_{ni}(t)}{dt} = \epsilon F_7(t) + \frac{P_{nu}(t)}{\gamma_{nb} x_u(t)} F_4(t) + \frac{P_{gi}(t)}{\gamma_{gb} x_i(t)} F_9(t) - \frac{P_{ni}(t)}{\gamma_{nb} x_i(t)} \times (F_8(t) + F_{10}(t)) \quad (7)$$

$$\frac{dP_{gi}(t)}{dt} = \frac{P_{gu}(t)}{\gamma_{gb} x_u(t)} F_6(t) - \frac{P_{gi}(t)}{\gamma_{gb} x_i(t)} \times (F_9(t) + F_{11}(t) + F_{13}(t)) \quad (8)$$

$$\frac{dP_{gv}(t)}{dt} = \frac{P_{ni}(t)}{\gamma_{nb} x_i(t)} F_{10}(t) - \frac{P_{gv}(t)}{\gamma_{gv} v(t)} F_{12}(t) \quad (9)$$

The total flows between compartments (F_i) are derived from the population submodel (Eqns. 1–3) and are given by:

$$F_1(t) = (\gamma_{nb} + \gamma_{gb}) \mu x_u(t)$$

$$F_2(t) = \gamma_{nb} m_u x_u(t)$$

$$F_3(t) = \gamma_{gb} \mu x_u(t)$$

$$F_4(t) = \gamma_{nb} r_v(t)$$

$$F_5(t) = \gamma_{gb} m_u x_u(t)$$

$$F_6(t) = \gamma_{gb} r_v(t)$$

$$F_7(t) = F_{10}(t) - F_9(t) - \gamma_{nb} r_v(t - \tau)\, e^{-m_i \tau}$$

$$F_8(t) = \gamma_{nb} m_i x_i(t)$$

$$F_9(t) = \alpha \gamma_{gb} r_v(t - \tau)\, e^{-m_i \tau}$$

$$F_{10}(t) = \gamma_{gv} \rho r_v(t - \tau)\, e^{-m_i \tau}$$

$$F_{11}(t) = \gamma_{gb} m_i x_i(t)$$

$$F_{12}(t) = \gamma_{gv}(r_v(t) + m_v v(t))$$

$$F_{13}(t) = (1 - \alpha) \gamma_{gb} r_v(t - \tau)\, e^{-m_i \tau}$$

and

$$\epsilon = \begin{cases} \sigma & \text{if } F_7(t) \geq 0 \\ \dfrac{P_{ni}(t)}{\gamma_{nb} x_i(t)} & \text{if } F_7(t) < 0 \end{cases}$$

where the terms γ_{nb}, γ_{gb}, and γ_{gn} represent cellular concentrations of nucleotides and nucleic acids in bacteria and in the viral genome, respectively, and σ is the fraction of ^{32}P-labelled phosphate in the culture medium. Values for both γ_{nb} and γ_{gb} are based on Escherichia coli composition [13], while γ_{gv} is based on a viral genome size of 50 kb ([11] and this study). To examine host genome degradation on label dynamics, an adjustable parameter a was introduced to modulate flows $F_9(t)$ and $F_{13}(t)$ to specify between 0% ($\alpha = 0$) and 100% ($\alpha = 1$) nucleic acid hydrolysis. The flow $F_7(t)$ was introduced to account for either de novo nucleotide synthesis when utilisation of host genome is small (small α) or excretion of excess nucleotides when degradation of host genome exceeds viral genome synthesis requirements (large α).

Dynamics of label incorporation were obtained by numerically integrating the seven state equations for different values of α. Label enrichment rate was found to be strongly dependent on extent of host genome degradation and specific growth rate but only weakly dependent on γ_{nb}, γ_{gb} and γ_{gv} (data not shown).

Results

Kinetics of phage growth and radiolabelling

The employed fractionation procedure of radiolabelled samples resulted in phage genomes clearly separated from other radioactive material, and thus removed most other phosphorus containing compounds in the sample (Fig. 3). The titre of PFUs showed a gradual increase with time within 4 h of infection and was paralleled by the increase in radioactivity in the phage DNA (Fig. 4). PFUs and radioactivity in phage DNA was found to be linearly correlated ($P < 0.002$, $r^2 > 0.93$) for all three phage isolates, with the exception of the last 2 h of the MØ14167 experiment, where PFUs (infectivity) declined, despite a continuing increase in newly formed phage genomes packed in protein capsids. A 1 h delay in the increase in ^{32}P in the phage genome relative to PFUs was observed for all three PHS (Fig. 4). This delay is obscured in Panel A because of the scale used for the high yield of phage. Net growth rates of the host bacteria (based on changes in optical density) were low during the

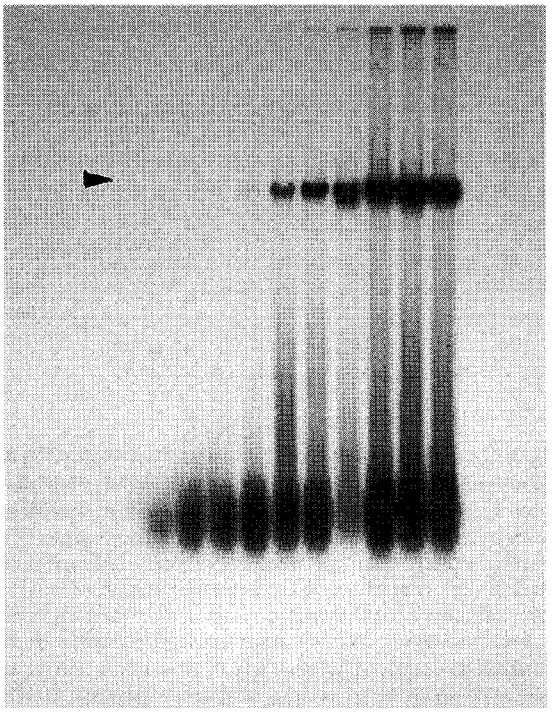

Fig. 3. Autoradiograph of samples from ^{32}P labelling experiment with PHS MØ21/50 after separation by agarose gel electrophoresis (corresponding to Fig. 4A). Lanes 1 to 11 show sequentially samples taken hourly from 0 to 11 h. The arrow indicates the position of MØ21/50 DNA marker.

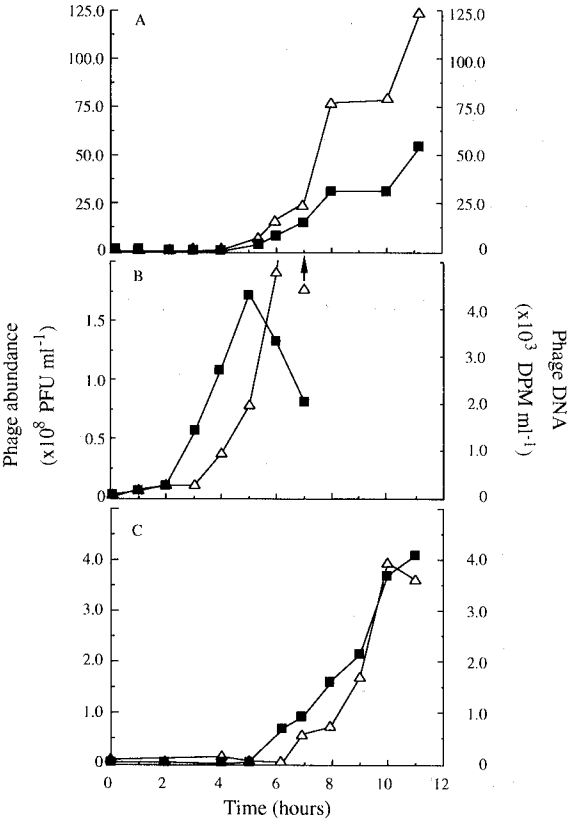

Fig. 4. Growth and radiolabelling of marine bacteriophages in culture experiments. Growth of phage determined by direct plating (PFU ■) and ^{32}P in the phage genome fractionated by gel electrophoresis (△), as in Fig. 3. 1 (a) PHS 21/50, (B) PHS 14/67, (C) PHS 21/43. The last radioactivity estimate in the PHS14/67 experiment corresponded to 13.2×10^3 dpm ml^{-1}.

experiments, corresponding to a doubling time of 0.05 h^{-1} (Fig. 1). Overall, incorporation of ^{32}P into phage DNA gave an accurate relative measure of phage growth under culture conditions.

Differential fractionation of phage and host bacteria

Filtration (0.2 μm) of autoclaved seawater samples spiked with marine phage isolates gave overall high recoveries of phage (Table 2). Average recovery of phage was 91% (95% C.I. ± 24). Recoveries were not statistically different from each other according to a one-way analysis of variance (ANOVA) ($P = 0.081$); however, correction for filtration losses in the labelling experiments was still done specifically for each phage. By direct plating it was shown that the viable count of bacterial cells was reduced to < 0.1 colony forming units ml^{-1} ($< 0.05\%$ of initial CFU) by the filtration procedure.

Table 2

Recovery of three marine phages after a filtration through a 0.22 μm Acrodisc®, and precipitation with ammonium sulphate, respectively

Treatment	Phage					
	MØ21/50		MØ21/43		MØ14/67	
	Mean	±SD	Mean	±SD	Mean	±SD
Filtration	0.81	0.09	0.92	0.21	1.00	0.09
Precipitation	0.92	0.05	0.85	0.24	0.51	0.10

Each phage type was seeded in a sterile sea water sample to a final concentration of 3×10^3 ml^{-1}. Phage titre was determined by plaque assay. Results are given as the average fraction of the phage recovered based on six replicates.

All three phage isolates could be precipitated with ammonium sulphate with appreciable recoveries (Table 2). The recovery was found to be phage specific (one-way ANOVA, $P = 0.001$) with the lowest recovery obtained for isolate MØ14167 of 51%. Thus, precipitation with this method resulted in a 2-fold difference in recovery depending on phage type. Average recovery was 76% (95% C.I. $\pm$ 54); however, corrections for loss were made individually for each phage in the labelling experiments. Dissolved DNA (MØ21/50 genome) did not precipitate under these conditions (data not shown), which was expected since DNA cannot be salted out at ammonium sulphate concentrations below 75% [9,14]

Modelling

The developed population sub-model well described the bacterial and phage dynamics in the experimental system (Fig. 1). The composite model predicted that the specific radioactivity of the phage DNA should rapidly approach the maximum theoretical value when nucleotides were provided by de novo synthesis and the host nucleotide pool only (i.e., host nucleic acids not hydrolysed, Fig. 5, curve B). The specific activity amounted to 68% of the maximum theoretical value already at the onset of the rise period of the phage population in this scenario. Simulating the other extreme (i.e., host genome and RNA hydrolysed for nucleotides), a gradual linear increase in specific radioactivity in the phage genome with time was observed (Fig. 5, curve C). When using host nucleic acids, the specific radioactivity reached 13×10^{-6} dpm PFU^{-1} after 10 h, 22% of that observed when only free nucleotides were used. Therefore, the model predicted that phage DNA specific activity and its kinetics was clearly dependent on whether nucleotides were synthesised de novo, or generated by hydrolysis of host nucleic acids, at the experimentally observed net bacterial growth rates. The fraction of the phage genome labelled when host nucleic acids were used as a nucleotide precursor pool was found to be sensitive primarily to the specific growth rate of the host cells. The pool size of the nucleoside monophosphate pool could be changed 100-fold to unreasonably high or low

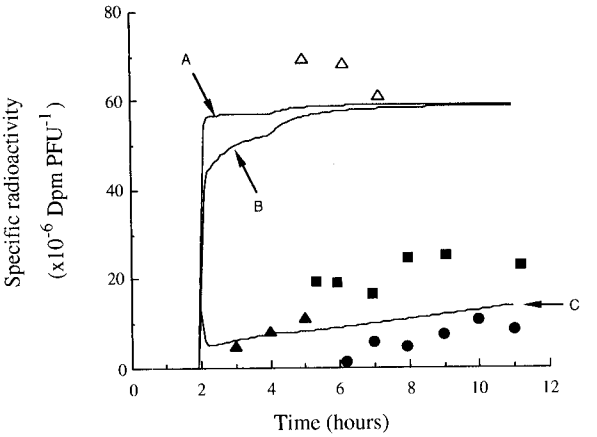

Fig. 5. Kinetics of the phage DNA specific activity during the culture experiments. Lines show results from simulations based on the model. (A) Prelabelled bacteria in radioactive medium, simulating expected kinetics of the phage DNA specific activity when all phosphorus pools are uniformly labelled (i.e., control for phage genome size and unexpected losses of phage). (B) Unlabelled bacteria simulating utilisation of host nucleotide and de novo nucleotide synthesis. (C) Unlabelled bacteria simulating use of host DNA, RNA, and nucleotide pool, but no de novo nucleotide synthesis. Markers show experimental data based on the rise period of the phages in Fig. 4. △, specific activity of phage DNA when grown on prelabelled cells in radioactive medium (PHS 21/50). Solid symbols represent phage grown on unlabelled host cells in radioactive medium for phage 21/50 (■), 21/43 (●) and 14/67 (▲).

values, without seriously affecting the percent of the genome labelled. The dependence of the phage genome specific activity on host cell specific growth rate showed a hyperbolic function (Fig. 6). At a specific growth rate of 0.2 h^{-1}, the model predicted 69% labelling of the phage genome 11 h after addition of radioisotope, when host nucleic acids were allowed as a nucleotide source. The data could be fitted ($r^2 > 0.9$) to the equation:

$$Sa_{rel} = 1 - \exp[-(at + b)\mu] \qquad (10)$$

where SA_{rel} is the relative specific activity of the phage genome, μ the host cell specific growth rate and a is a constant estimated to be 0.466; b a constant estimated to be 0.617 and t represents time after addition of radiolabel. The relative specific activity obviously depends on the time of sampling after addition of radiolabel with higher

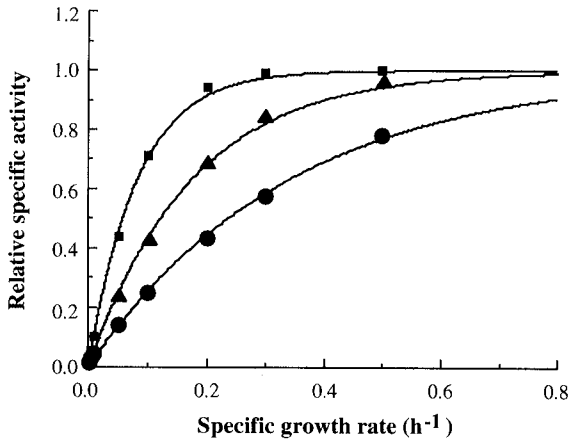

Fig. 6. Dependence of phage DNA specific activity on bacterial specific growth rates, assuming all nucleotides to be derived from the host DNA, RNA and free nucleotides. The fraction of the phage genome labelled after 5 (●), 11 (▲), and 25 h (■), respectively, was estimated at nine different bacterial specific growth rates, based on the model. The relative specific activity of the phage genome is shown as a fraction of the specific activity of the growth medium.

values being obtained after longer times according to the curves in Fig. 6.

Specific activity of phage DNA

The specific activity of the phage genomes during the experiments with unlabelled host cells was in accordance with the scenario where hydrolysed host DNA and RNA comprised the major source of nucleotides for phage DNA synthesis (Fig. 5). Despite that a slight difference between the isolates in absolute values and rate of increase in specific activity was observed, all PHSs were best approximated to the curve that simulated hydrolysed host nucleic acid as the main source of nucleotides for phage DNA synthesis. Only samples collected during the rise period of the phage population in the different experiments were used, since it is only after release of phages that the direct plating technique gives a good approximation of the phage titre, and radioactivity in phage genomes becomes representative of essentially free phage with the method employed. Due to an apparently high inactivation rate of MØ14/67 phages at the end of the experiment, only three samples gave reliable estimates of the specific radioactivity. Mean specific activity in the individual experiments was 2.1×10^{-5}, 0.83×10^{-5} and 0.65×10^{-5} dpm PFU^{-1}, for PHS 21/50, 14/67 and 21/43, respectively (Table 3). On average, this was only 21% (95% C.I. ± 5.9) of the specific activity expected, based on the actual $^{32}P/^{31}P$ ratio in the medium and the phage genome size. The corresponding value when host cells were prelabelled with ^{32}P was close to the theoretical maximum value (102%; Table 3). Thus, samples from the experiment with uniformly prelabelled host cells fell close to the specific activity predicted by the model (Fig. 5, curve A).

Table 3

Effect of isotope dilution in culture experiments with marine phage-host systems

Phage	Genome size (base pairs) ($\times 10^3$)	Slope coeff. (SA) [a] (dpm pfu^{-1}) ($\times 10^{-5}$)	$[^{31}PO_4^{3-}]$ (μM)	SA_{calc} (dpm $phage^{-1}$) ($\times 10^{-5}$)	SA_{rel} (%)
MØ21/50 [b]	62.8	6.63	72	6.49	102
MØ21/50	62.8	2.12	57	8.19	26
MØ14/67	36.9	0.83	72	3.82	22
MØ21/43	34.9	0.65	57	4.55	14
Average [c]	44.9				21

The maximum theoretical specific activity (SA_{calc}) was calculated from the genome size and specific activity of $^{32}PO_4^{3-}$ in the medium. The relative labelling of the phage genome (SA_{rel}) was calculated from the observed mean specific activity of the phage genome (SA; Fig. 5), and SA_{calc}. Samples were corrected for losses at the filtration and precipitation step. Determined genome sizes and phosphate concentration in the medium are also given.

[a] Mean value from the experiments in Fig. 5

[b] Host cells prelabelled with $^{32}PO_4^{3-}$ overnight (≈ 7 generations).

[c] Average of the three PHS studied.

The good agreement with the maximum specific activity obtained with uniformly labelled host cells indicated that corrections for recoveries were adequate and that other sources of phosphorus (i.e., organic-P) in the medium did not influence the actual $^{32}P/^{31}P$ ratio. In short, the specific activity of phage genomes consistently amounted to a small fraction of the specific radioactivity of the external medium and increased gradually during growth with ^{32}P-phosphate under culture conditions.

Discussion

Nucleotide metabolism

The low and gradually increasing specific activity of the phage genomes was consistent with a scenario where the majority of nucleotides used during phage DNA synthesis were derived from degraded nucleic acids (i.e., DNA and RNA) of the host cell (Fig. 5). This observation was consistent among the three marine phage isolates investigated. We are not aware of other reports on the origin of phosphorus in marine phages. For the T-even phages of enteric bacteria it has been shown that 70–80% of the phage DNA phosphorus is derived from the surrounding medium, suggesting that most of the nucleotides used for phage DNA synthesis came from de novo synthesis (i.e., phosphorylation of nucleosides) ([5], and references therein). The remaining nucleotides were derived from hydrolysed host nucleic acids. It is possible that enteric phages from nutrient rich environments have a different strategy for nucleotide metabolism than marine phages adapted to growth in oligotrophic environments. However, Kozloff and Putnam [5] did not take the bacterial specific growth rate into account in their interpretation of de novo synthesis; high specific growth rate (i.e., replication rate) of *E. coli* in their experiment may have resulted in high specific activity of the phage genome, despite predominant use of nucleic acids as the major nucleotide source, as suggested by our model (cf. Fig. 6).

The DNA plus RNA content of an average-sized (0.050 μm^3) marine bacterium is estimated to be 5.3 fg cell^{-1} [15], which would be sufficient to produce 118 phage genomes per cell, assuming 0.045 fg (phage genome)$^{-1}$ (Table 3, [11]). Thus, host nucleic acids alone are sufficient to support a burst size which is within the range actually reported for many phages (10–300 phages cell^{-1}) and realistic under oligotrophic conditions [11,12]. It is therefore reasonable to propose that a majority of nucleotides in the phage genome were derived from host DNA and RNA. Since this calculated yield is within the range of burst sizes reported, we may also speculate that the amount of intracellular host nucleic acid could limit the yield of infective phage per cell.

The ability of a phage to utilise host nucleic acids as a source of nucleotides appears to be coupled to the presence of phage encoded endo- and exonucleases specific for host nucleic acids [16]. Assuming that the nucleotide metabolism of marine phages is similarly coupled to the phage genotype, it is plausible that our observations from cultures can be extrapolated to the natural environment. It may be speculated that extensive use of host nucleic acids for phage DNA synthesis is a common metabolic strategy of marine phages in general. The low variability in fraction of phosphorus derived from nucleic acid found between the phage isolates in our study (95% C.I. $\pm$ 5.9; Table 3), and the possible advantage of using available intracellular nucleic acids in a nutrient poor environment would argue for this possibility. It is conceivable that the nucleotide metabolism of phages vary with phage-host system, as an adaptation to the nutrient status of the natural growth environment. An ecological consequence of extensive degradation of the bacterial DNA by infecting phage, is that the ensuing lysis of bacteria will not contribute as much DNA to the dissolved pool as previously suggested [17]. The approach and model used by us to investigate the source of nucleotides of phage nucleic acid can readily be applied to other marine phage-host systems to test our hypothesis.

Accuracy of phage DNA determination

The electrophoretic fractionation of the precipitated samples resulted in phage DNA bands clearly separated from other phosphorus contain-

ing compounds (Fig. 3). Correction for losses due to filtration and precipitation resulted in quantitative determination of the amount of newly formed phage DNA, as shown by the good agreement between experimental and theoretical specific activity of phage DNA in experiments with uniformly pre-labelled cells (Fig. 5, Table 3). No indications of marked losses of phage DNA with the developed protocol was therefore observed.

A common discrepancy in the kinetics between PFUs and ^{32}P in the phage genome was a short lag in the latter, following the rise in PFUs (Fig. 4). This was likely due to the initially low specific activity in the precursor nucleotide pools during the earliest part of phage DNA synthesis. Although we expect a non-synchronised phage population under field conditions, a similar lag period may be expected due to both equilibration of radiolabel in nucleotide pools and the time needed for assembly and release of the complete virions. Using the present protocol we measure the DNA of released free phage particles, while intracellular phage DNA or dissolved uncoated phage DNA are not included. Therefore, monitoring of the accumulation of radiolabelled phage DNA, fractionated by gel electrophoresis gave an accurate relative measure of phage growth for the three marine phage isolates investigated.

Isotope dilution in the natural environment

By comparing the sensitivity of different parameters in our model we could demonstrate that the specific growth rate of the host strongly determined the extent of isotope dilution, when nucleotides were predominantly derived from host DNA and RNA (Fig. 6, Eqn. 10). Assuming that the isolation procedure of phages is not selective in terms of nucleotide metabolism, statistically 95% of the marine phages may be expected to have a SA_{rel} less than 27% and therefore derive most of their phosphorus from nucleic acid (i.e., mean plus one 95% C.I., Table 3). In field experiments including radiolabelling of phages, average phage genom size would be 3-fold lower than found for phages in general if not taking isotope dilution into account [11,18]. This suggest a 3-fold isotope dilution in the phage nucleic acid in good agreement with the results of the three phage isolates in this study. Based on these considerations it may be proposed that the metabolic strategy observed for the studied phage isolates is common in the marine phage community.

When phages with nucleotide metabolism similar to our three isolates dominate the phage community, the extent of isotope dilution in the field will depend on the specific growth rate of the host bacterium. Although specific growth rate of the bacterial community may be just slightly lower than that observed during our radiolabelling experiments, it is conceivable that the specific growth rate of individual bacterial populations in situ may be markedly different. According to our model, a 8-fold decrease in isotope dilution is expected (11 h scenario) if the specific growth rate is changed from 0.005 h^{-1} to 0.05 h^{-1}, a probable range in natural environments. Therefore, the phage type composition and growth rate of the host bacteria in situ, will influence the extent of isotope dilution when radiolabelling natural phage populations.

Based on the results presented above we conclude that marine phages may derive the majority of their nucleotides from the nucleic acids of the bacterial host. This metabolic strategy may be common in the marine phage community, and contrast the origin of nucleotides in coli-phages, suggested to be mainly derived by de novo synthesis. The capacity of marine phage to use the intracellular resources of the host bacterium may be an evolutionary adaptation promoted by the low ambient concentration of substrate generally found in the marine environment.

Acknowledgements

We are indebted to Drs. Martínez and Cochlan for carefully reading and providing valuable comments on the final version of the manuscript. This work was supported by The US NSF through grants to F. Azam. J. Wikner was supported by grants from the Swedish Natural Science Research Council (B-PD 8583-308), the Sweden-America Foundation and the Kempe Foundation. J. Vallino was supported by grants from the Mellon Foundation.

References

1 Bergh, Ø., Børsheim, K.Y., Bratbak, G. and Heldal, M. (1989) High abundance of viruses found in aquatic environments. Nature 340, 467–468.

2 Cochlan, W.P., Wikner, J., Steward, G.F., Smith, D.C. and Azam, F. (1993) Spatial distribution of viruses, bacteria, and chlorophyll-a in neritic, oceanic and estuarine environments. Mar. Ecol. Prog. Ser. 97, 77–87.

3 Mathews, C.K. and Allen, J.R. (1983) Enzymes and proteins of DNA metabolism. In: Bacteriophage T4 (Mathews, C.K., Kutter, E.M., Mosig, G. and Berget, P.B., Ed.), pp. 59–70. American Society for Microbiology, Washington, DC.

4 Steward, G.F., Wikner, J., Cochlan, W.P., Smith, D.C. and Azam, F. (1993) Estimation of virus production in the sea: I. Method development Marine Microbial Foodwebs 6, in press.

5 Kozloff, L.M. and Putnam, F.W. (1950) Biochemical studies of virus reproduction: III. The origin of virus phosphorus in the *Escherichia coli* T_6 bacteriophage system. J. Biol. Chem. 182, 229–243.

6 Parsons, T.R., Maita, Y. and Lalli, C.M. (1984) A manual of chemical and biological methods for sea water analysis, p. 173. Pergamon Press, Oxford.

7 Sambrook, J., Fritsch, E.F. and Maniatis, T. (1989) Molecular cloning: A laboratory manual, Vols. 1, 2 and 3. Cold Spring Harbour Laboratory, Cold Spring Harbour.

8 Delbecco, R. and Ginsberg, H.S. (1988) Virology, p. 25. Lippincott Company, Philadelphia.

9 Ziai, M.R., Giordano, A., Armandola, E. and Ferrone, S. (1988) Purification by ammonium sulfate precipitation of bacteriophage Lambda gt11 DNA for restriction analysis of cloned cDNA inserts. Anal. Biochem. 171, 192–196.

10 Lenski, R.E. (1984) Dynamics of interactions between bacteria and virulent bacteriophage. In: Advances in microbial ecology (Marshall, K.C., Ed.), Vol. 10, pp. 1–44. Plenum Press, New York.

11 Ackermann, H.-W. and DuBow, M.S. (1987) Natural groups of bacteriophages, Vol. 2, p. 242. CRC Press, Boca Raton.

12 Heldal, M. and Bratbak, G. (1991) Production and decay of viruses in aquatic environments. Mar. Ecol. Prog. Ser. 72, 205–212.

13 Ingraham, J.L., Maaløe, O. and Neidhardt, F.C. (1983) Growth of the bacterial cell, p. 3. Sinauer Associates, Inc., Sunderland.

14 Freifelder, D. (1982) Physical biochemistry, p. 761. W.H. Freeman & Co., San Francisco.

15 Simon, M. and Azam, F. (1989) Protein content and protein synthesis rates of planktonic marine bacteria. Mar. Ecol. Prog. Ser. 51, 201–213.

16 Warner, H.R. and Snustad, D.P. (1983) T4 DNA nucleases. In: Bacteriophage T4 (Mathews, C.K., Kutter, E.M., Mosig, G. and Berget, P.B., Ed.), pp. 103–109. American Society for Microbiology, Washington DC.

17 Proctor, L.M. and Fuhrman, J.A. (1991) Roles of viral infection in organic particle flux. Mar. Ecol. Prog. Ser. 69, 133–142.

18 Steward, G.F., Wikner, J., Cochlan, W.P., Smith, D.C. and Azam, F. (1993) Estimation of virus production in the sea: II. Field results. Marine Microbial Food Webs 6, in press